IEEE Access
Multidisciplinary | Rapid Review | Open Access Journal

Received January 21, 2019, accepted February 11, 2019, date of publication February 21, 2019, date of current version March 26, 2019.

Digital Object Identifier 10.1109/ACCESS.2019.2900566

Novel Tri-Band High-Temperature Superconducting Bandpass Filters Using Asymmetric Shunted-Line Stepped-Impedance Resonator (SLSIR)

HAIWEN LIU[1], (Senior Member, IEEE), YIFAN WANG[2], PIN WEN[1,2], AND SHAOYONG ZHENG[3], (Senior Member, IEEE)

[1]School of Electronic and Information Engineering, Xi'an Jiaotong University, Xi'an 710049, China
[2]School of Information Engineering, East China Jiaotong University, Nanchang 330013, China
[3]School of Electronics and Communication Engineering, Sun Yat-sen University, Guangzhou 510275, China

Corresponding author: Pin Wen (wenpin925@hotmail.com)

This work was supported by the National Natural Science Foundation of China (No. U1831201, 61728106), the Natural Science Foundation of Jiangxi Province of China under (No. 2017ACB20019), and the Science & Technology Project and Research Program of Jiangxi Province of China (No. 2016BCB18010, 20171BBE50056, 20181BCB24010).

ABSTRACT In this paper, a tri-band high-temperature superconducting (HTS) bandpass filter (BPF) is proposed with a pair of asymmetric shunted-line stepped impedance resonators (SLSIRs). Compared with the conventional SIRs, the proposed asymmetric SLSIR has more degrees of freedom in controlling multi-mode operating characteristics. Moreover, design graphs for the relationship of electric characteristic parameters and the resonant frequency ratio are built and applied to multiband device design. For demonstration, a two-order tri-band HTS BPF is well designed with center frequencies of 1.575/2.4/3.5 GHz. The external quality factor and the coupling coefficient have also been analyzed to satisfy the bandwidth of the BPF. The designed filter is fabricated on the YBCO superconducting material and measured under superconducting conditions (at the temperature of 77 K). The measurement results are in good agreement with the simulation results, indicating that the insertion loss of the three passbands is about 0.1 dB, showing the advantage of in-band insertion loss.

INDEX TERMS Asymmetric shunted-line stepped-impedance resonator (SLSIR), bandpass filter (BPF), high-temperature superconducting (HTS), tri-band.

I. INTRODUCTION

With the increasing development of multi-service wireless communication networks, a single transceiver system working at multiple frequency bands has attracted great much attentions. It is critical for bandpass filter to offer multi-band operation while at the same maintaining compact size and high selectivity. Several methods have been utilized to design multiband BPF. One is multiple individual BPFs with different passbands are assembled. In [1]–[4], several sets of resonators are parallel connected to form multiple filtering paths with common feeding structure to produce multi-band BPFs. In [1] and [2], stepped impedance resonators (SIRs) are parallel assembled to achieve tri-band BPF with high selectivity. The SIRs and stub-loaded resonators (SLR) are cascaded in parallel to produce tri-band BPFs in [3]. Multipath-embedded SIRs are adopted to reduce the circuit size with high passband selectivity and low insertion loss [4]. Nevertheless, these BPFs always suffer from enlarged overall area or size because of multiple resonator units.

In order to reduce the circuit size, dual-layer technique is used to design multi-band BPF. In [5], a double-layered substrate design utilizing four pairs of microstrip SIRs on the top and middle metal layers to design the four-band BPF is proposed. The third approach is using multi-mode resonators (MMRs) for multi-band BPFs design. For example, modified quarter-wavelength SIRs are used in [6] to realize miniature dual-band bandpass filter. Besides, SLR is

The associate editor coordinating the review of this manuscript and approving it for publication was Yingsong Li.

presented to achieve tri-band BPF with simple configuration [7], [8]. To improve the design freedom of the filter circuit, unequal-length shunted-line SIR (SLSIR) with more degrees of freedom is discussed to design dual-band BPF [9]. Compared to the conventional SIR, SLSIR is flexible to control the resonant frequencies of the resonator. However, due to the low Q factor of the SLSIR, the multi-band BPF described above on a standard PCB substrate has a relatively large insertion loss in the band.

It is known that high temperature superconducting techniques can be used to produce microwave devices with very low insertion loss to meet the needs of the application. At present, some experts and scholars have tried to design BPF with high temperature superconducting technology. [10]–[16]. In [10], a single-band HTS bandpass filter using CPW quarter-wavelength spiral resonators was reported. In [11], stub-loaded resonators are used to design a high-order dual-band superconducting filter. Tri-band HTS filters are designed by using asymmetric tri-section stepped impedance resonator (TSIR) in [12]. Embedded SLRs are used in [13] to improve the selectivity of the tri-band. Multiple SLRs, coupled-line stepped-impedance-resonator (C-SIR) and stub-loaded meander line resonators are adopted in [14]–[16] to design tri-band BPF, respectively. All of the superconducting filters mentioned above have the advantage of extremely low insertion loss. However, the resonator should be improved to achieve more design freedom to meet the filter requirements of future communication systems.

In this paper, an asymmetric SLSIR with multiple design freedoms is proposed. Three controllable resonant modes are generated by the asymmetric SLSIR to form a tri-band frequency response. Resonant characteristics of the proposed resonator have been well investigated and several design graphs have been drawn to guide the filter design. Finally, a tri-band filter was fabricated on the YBCO superconducting material and measured at the temperature of 77K. There is good agreement between simulation and measurement results.

II. IMPLEMENTATION OF THE TRI-BAND HTS BPF

A. RESONATANCE ANALYSIS OF SLSIR

Compared with a conventional SIR, a schematic view of the proposed asymmetric SLSIR is shown in Fig. 1(a). Its characteristic admittances and the corresponding electrical lengths are represented as Y_1, Y_2, Y_3 and θ_1, θ_2, θ_3, respectively. The structural difference between the two resonators is that the proposed SLSIR is loaded with an asymmetric shunted-lines resonator (ASLR) at both ends to replace the specific TL section $\theta_2\prime$ of the conventional SIR. Thus, the asymmetric SLSIR has more degrees of freedom to adjust the resonance modes for multi-band design.

The proposed SLSIR is symmetric structure along the symmetrical interface. Then, the even- and odd-mode analysis method is used to analyze the resonance characteristic of the SLSIR. Under odd-mode excitation or even-mode excitation,

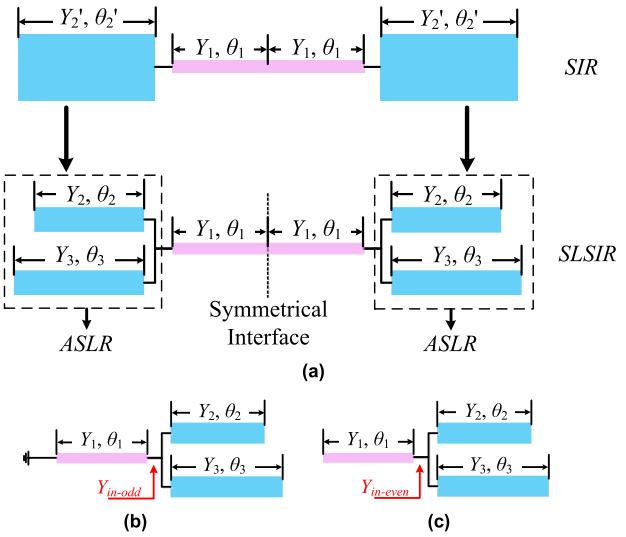

FIGURE 1. (a) Transmission line model of the asymmetric SLSIR. (b) Odd-mode equivalent circuit. (c) Even-mode equivalent circuit.

its equivalent circuits are given in Fig. 1(b) and Fig. 1(c), respectively. The input admittance of the proposed SLSIR under odd-mode excitation and even-mode excitation are deduced as follows:

$$Y_{in-odd} = jY_3 \tan\theta_3 + jY_2 \tan\theta_2 - jY_1 \cot\theta_1 \quad (1)$$

$$Y_{in-even} = jY_3 \tan\theta_3 + jY_2 \tan\theta_2 + jY_1 \tan\theta_1 \quad (2)$$

Letting the imaginary part of Y_{in-odd} equals to zero, the odd-mode resonance condition of the proposed SLSIR is obtained as:

$$Y_3 \tan\theta_3 + Y_2 \tan\theta_2 = Y_1 \cot\theta_1 \quad (3)$$

Similarly, the even-mode resonant condition of the proposed SLSIR with open-circuit structure in Fig. 1 (c) is derived by:

$$Y_3 \tan\theta_3 + Y_2 \tan\theta_2 = -Y_1 \tan\theta_1 \quad (4)$$

Then, the three resonant frequencies (the first odd-mode frequency, f_{o1}, the first even-mode frequency, f_{e1}, and the second odd-mode frequency, f_{o2}) of the SLSIR can be obtained from (3) and (4).

Based on Eq. (3) and (4), the two odd-mode resonant frequencies (f_{o1} and f_{o2}) and one even-mode resonant frequency (f_{e1}) of the proposed SLSIR are chosen to form the three passbands. Then, the resonant condition of the odd- and even-mode resonances can be rewritten as:

$$K_2 \tan\frac{f_{o1}}{f_0}\theta_3 + \tan\frac{f_{o1}}{f_0}\theta_2 = K_1 \cot\frac{f_{o1}}{f_0}\theta_1. \quad (5)$$

$$K_2 \tan\frac{f_{o2}}{f_0}\theta_3 + \tan\frac{f_{o2}}{f_0}\theta_2 = K_1 \cot\frac{f_{o2}}{f_0}\theta_1 \quad (6)$$

$$K_2 \tan\frac{f_{e1}}{f_0}\theta_3 + \tan\frac{f_{e1}}{f_0}\theta_2 = -K_1 \tan\frac{f_{e1}}{f_0}\theta_1 \quad (7)$$

For simplicity, the admittance ratios $K_1 = Y_1/Y_2$ and $K_2 = Y_3/Y_2$ are assumed. In this work, all of the electrical lengths are calculated at $f_0 = 3.5$ GHz.

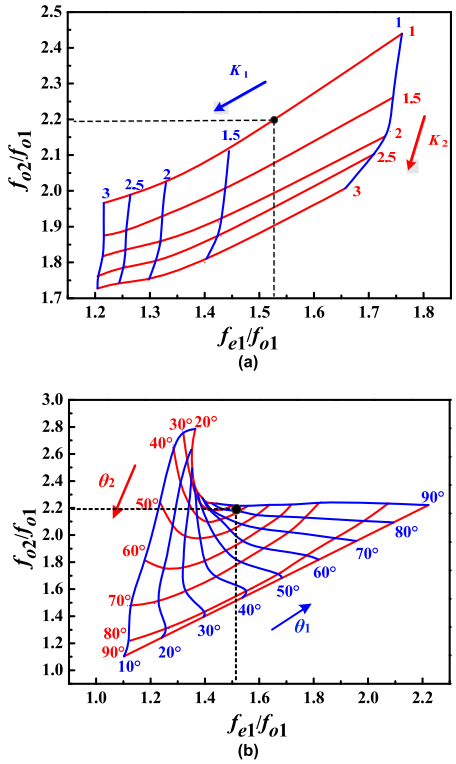

FIGURE 2. (a) Frequency ratios of f_{o2}/f_{o1} versus f_{e1}/f_{o1} with different K_1 and K_2 under the condition of specified $\theta_2 = 24.8°$ ($\theta_3 = 155.2°$) and $\theta_1 = 75.7°$ and (b) Frequency ratios of f_{o2}/f_{o1} versus f_{e1}/f_{o1} with different θ_2 and θ_1 under the condition of specified K_2 =1 and K_1 =1.4.

Based on Eq. (5), (6) and (7), it is found that the SLSIR can produce multiple resonant frequencies with different electrical lengths and admittance ratios. To further clarify the relationship between the resonant frequencies and key parameters of resonator, two graphs are plotted in Fig. 2 based on Eq. (5), (6) and (7).

Furthermore, the design graphs with specified electrical length (θ_1 and θ_2) or admittance ratios (K_1 and K_2) can be plotted. To simplify, $\theta_2 + \theta_3$ is set equal to a half wavelength. As shown in Fig. 2(a), the relation of f_{o2}/f_{o1} versus f_{e1}/f_{o1} are presented with different K_1 and K_2 with specifying $\theta_1 = 75.7°, \theta_2 = 24.8°$ and $\theta_3 = 155.2°$. As can be seen from Fig. 2(a), two frequency ratios both appear to be smaller values as K_1 and K_2 becomes large. When K_1 keeps unchanged and K_2 is enlarged, f_{o2}/f_{o1} is increased. Similarly, as shown in Fig. 2(b), the relation of f_{o2}/f_{o1} versus f_{e1}/f_{o1} are depicted with different θ_1 and θ_2 by setting the $K_1 = 1.4$ and $K_2 = 1$. Although the illustrated tuning ranges of f_{o2}, f_{e1} and f_{o2} in Fig. 2 are limited, more design data can be extracted by choosing different combinations of θ_1, θ_2, K_1 and K_2 when needed. Moreover, once the design specification about the tri-band filter's resonant frequencies are chosen, the specified electrical lengths (θ_1 and θ_2) and the characteristic admittance ratios (K_1 and K_2) of resonator can be found from Fig. 2. From the above analysis, it can be seen that asymmetric SLSIR has higher design freedom than conventional SIR, which can flexibly satisfy the design requirements of the tri-band BPF.

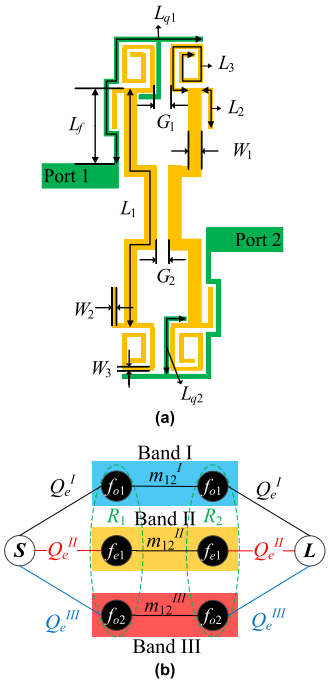

FIGURE 3. (a) Configuration of the proposed tri-band BPF. (L_1 =13.6, L_f =3.5, L_2 =2.3, L_3 =15.15, L_q =4.95, $W_2 = W_3$ =0.2, W_1 =0.45, G_1 =0.9, G_2 =0.7. Unit: mm). (b) Coupling diagram of the two-order tri-band filter.

B. FILTER DESIGN

For demonstration, the proposed SLSLR is applied to design a tri-band HTS BPF for Global Positioning System (GPS), Wireless Local Area Networks (WLAN) and 5G applications. Two-order Chebyshev tri-band BPF centered at 1.575 (f_{o1}), 2.4 (f_{e1}), and 3.5 (f_{o2}) GHz with 3-dB fractional bandwidths $\Delta_1 = 4.9\%, \Delta_2 = 3.75\%, \Delta_3 = 2.9\%$ is designed. So, two frequency ratios are calculated as: $f_{e1}/f_{o1} = 2.4/1.575 \approx 1.52$ and $f_{o2}/f_{o1} = 3.5/1.575 \approx 2.22$. With the specified $\theta_1 = 75.7°, \theta_2 = 24.8°$ and $\theta_3 = 155.2°$ in Fig. 2(a), $K_1 = 1.4$ and $K_2 = 1$ are found and indicated by a black spot. Similarly, as shown in Fig. 2(b) for the specified $K_1 = 1.4$ and $K_2 = 1$, the frequency ratios of f_{o2}/f_{o1} versus f_{e1}/f_{o1} are depicted with different θ_2 and θ_1. Thus, it is easy to design tri-band filter's resonant frequencies with the specified electrical lengths (θ_2 and θ_1) from Fig. 2(a) and the characteristic admittance ratios (K_1 and K_2) from Fig. 2(b).

To further reduce the circuit size, the resonators are folded as shown in Fig. 3. According to above design theory and then tuned design by *EM simulator*, the final dimensions noted in Fig. 3 are obtained as follows: $L_1 = 13.6, L_f = 3.5, L_2 = 2.3, L_3 = 15.15, L_q = 4.95, W_2 = W_3 = 0.2, W_1 = 0.45, G_1 = 0.9, G_2 = 0.7$ (Unit: mm).

The following steps are to determine the physical size of the coupling gaps between resonators and the input/output feeding structure according to the theory values of coupling coefficients and external quality factors (Q_e) by the *EM simulator*.

Fig. 3(a) is the configuration of the presented two-order tri-band BPF. And its coupling scheme is in Fig. 3(b), where nodes S and L denote input and output ports, respectively.

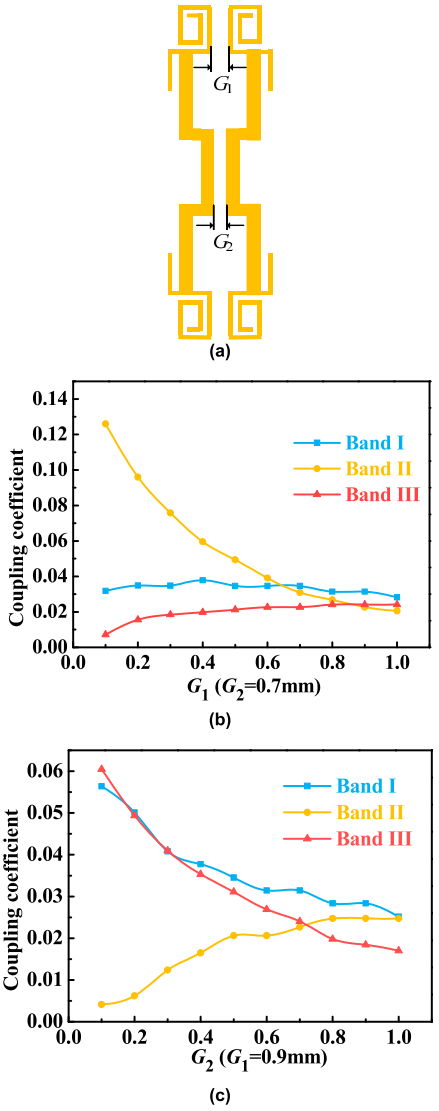

FIGURE 4. (a) Configuration of two coupled SLSIRs. Coupling coefficients as a function of the coupling spaces of (b) G_1 and (c) G_2.

R_1 and R_2 indicate the two order SLSIRs. There are three coupling paths in this coupling diagram, which is corresponding to the three passbands, Band I, Band II and Band III of the tri-band BPF. Three coupling paths can be used to control the fractional bandwidths of the three passbands.

The coupling coefficient can be calculated by the following formula:

$$M_{ij} = \frac{f_{p2}^2 - f_{p1}^2}{f_{p2}^2 + f_{p1}^2}. \tag{8}$$

where f_{p1} and f_{p2} are the lower and higher resonant frequencies of the coupled resonators, respectively.

Fig. 4 shows the extracted coupling coefficients of the BPF with varied gap widths G_1 (the distance between two ASLR) and G_2 (the distance between the high admittance portions of the resonator). When G_1 increases and G_2 keeps constant to 0.7 mm, the coupling coefficients of the second passband is reduced and the ones of the first and third passbands are almost unchanged. It means the coupling coefficient of

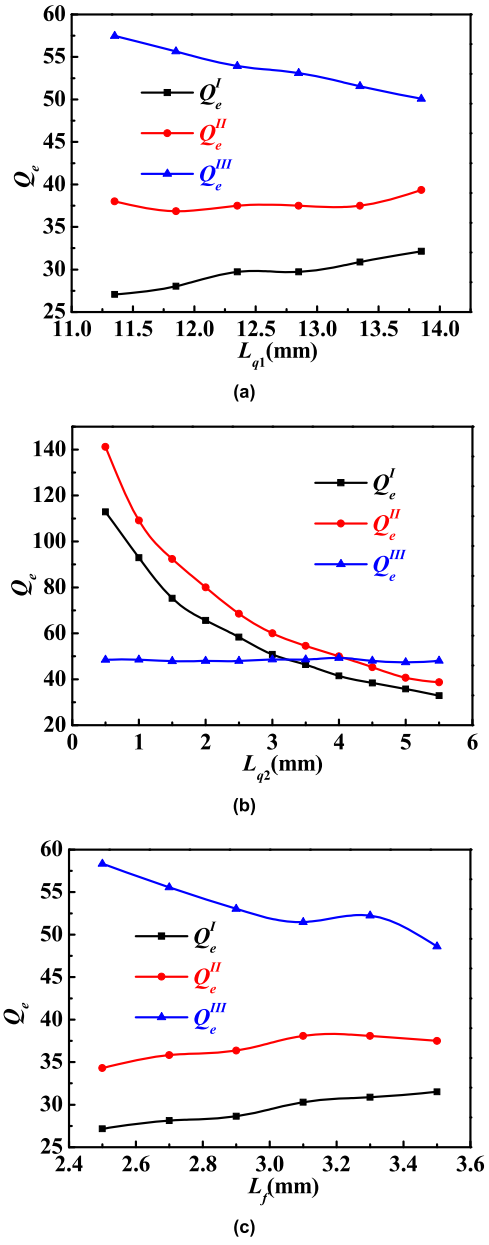

FIGURE 5. Simulated external quality factors of the three passbands with different coupled-line length L_{q1} (a) and L_{q2} (b) and feeding position L_f (c).

the second passband can be independently controlled by G_1. Contrastively, when G_2 increases and G_1 keeps constant to 0.9 mm, the coupling coefficients of the second passband is increased while the ones of the first and third passbands are decreased. Therefore, by adjusting G_1 and G_2, the coupling coefficients of the required bandwidth can be obtained.

The following is to determine the feeding structure of the proposed resonator. The Q_e value of the proposed filter can be extracted from the following expression:

$$Q_e = \frac{\omega_0}{\Delta\omega_{\pm 90^\circ}} \tag{9}$$

where ω_0 and $\Delta\omega_{\pm 90^\circ}$ represent the resonant angular frequency and the absolute bandwidth between the $\pm 90^\circ$ points of S_{11} phase response.

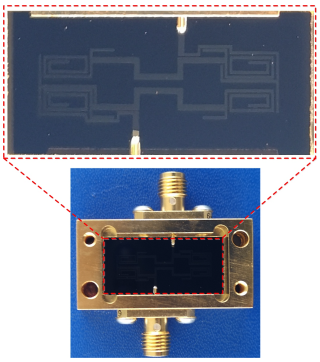

FIGURE 6. Photograph of the fabricated HTS circuit.

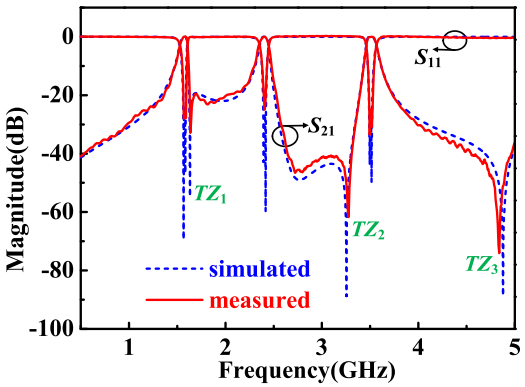

FIGURE 7. Frequency responses of the proposed tri-band HTS BPF.

Fig. 3(a) shows the feed structure of the proposed tri-band filter. From Fig. 5, proper combination of L_f, L_{q1} and L_{q2} can be chosen to meet the wanted external quality factors at three passbands. From Fig. 5, the external quality factors of three passbands, Q_e^I, Q_e^{II}, and Q_e^{III} could be tuned by changing L_f $L_{q1}$and L_{q2}. With the increase of L_f, Q_e^I and Q_e^{II} will also increase while Q_e^{III} decreases. The increase of L_{q2} will lead to a decrease of Q_e^I and Q_e^{II} when Q_e^{III} keeps almost constant. Based on the required values of Q_e^I, Q_e^{II} and Q_e^{III}, L_f, L_{q1} and L_{q2} are finally determined as 3.5 mm, 13.85 mm and 5.95 mm, respectively.

III. FABRICATION and MEASUREMENT

The proposed filter was fabricated on the MgO wafer with a double-sided YBCO film. The fabricated circuit is packaged in a metal shielded box for convenient measuring. Fig. 6 shows the photograph of the fabricated tri-band HTS bandpass filter. The overall size of the filter is 5.7 mm $\times$ 18.8 mm, and is about $0.076\lambda_g \times 0.26\lambda_g$ ($0.02\lambda_g^2$) despite feed lines (λ_g is the guided wavelength at the center frequency of the lowest passband).

The fabricated HTS filter was measured by an analyzer Keysight E5071C in a cryogenic cooler at the temperature of 77 K. A comparison between simulations and measurements is presented in Fig. 7, where the dashed lines and solid lines indicate the simulated and measured results, respectively. Fig. 8 is an enlarged picture of three passbands in the frequency response. As shown in Fig. 7 and Fig. 8, the measured passband frequencies are located at 1.575 GHz, 2.4 GHz and 3.5 GHz, respectively. The corresponding

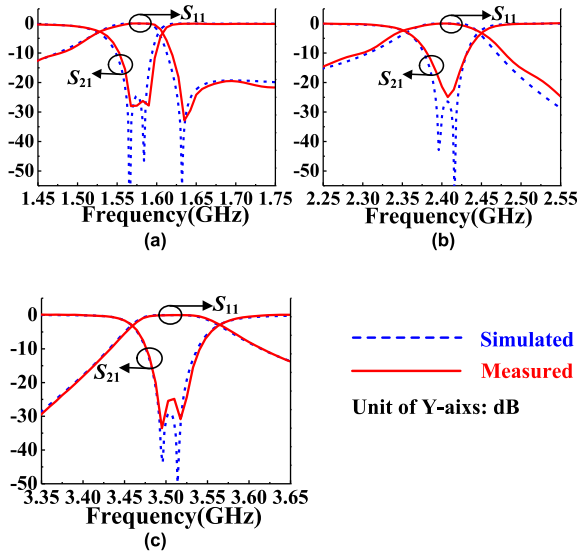

FIGURE 8. Enlarged scale in-band. (a) First passband. (b) Second passband, (c) Third passband.

3-dB fractional bandwidths are 5.2%, 4.25% and 2.7%. The rejection between the three transmission bands is better than 20 dB from 2.3 GHz to 5 GHz. The transmission zeros of TZ_1, TZ_2 and TZ_3 are created by the 0° feeding structure. The measured insertion losses within passbands are better than 0.1, 0.09 and 0.11 dB, which is attributed to the usage of HTS film material.

IV. CONCLUSION

A tri-band HTS BPF with good performance is realized with the asymmetric SLSIR in this paper. Compared with the conventional SIR, the proposed asymmetric SLSIR has more degrees of freedom in controlling multi-mode operating characteristics. The center frequencies of the three passbands can be adjusted by different electrical lengths and admittance ratio. Simulation and measured results are presented to verify the circuit design method. The proposed tri-band HTS BPF exhibits excellent performance with a minimum insertion loss of 0.1 dB for the three passbands. The above results prove that this design is quite suitable to fabricate high performance multi-band filters when high design flexibility is required.

REFERENCES

[1] F. C. Chen and Q. X. Chu, "Design of compact tri-band bandpass filters using assembled resonators," *IEEE Trans. Microw. Theory Techn.*, vol. 57, no. 1, pp. 165–171, Jan. 2009.

[2] B.-J. Chen, T.-M. Shen, and R.-B. Wu, "Design of tri-band filters with improved band allocation," *IEEE Trans. Microw. Theory Techn.*, vol. 57, no. 7, pp. 1790–1797, Jul. 2009.

[3] N. Sekiya and S. Sugiyama, "Design of tri-band superconducting bandpass filters with independently controllable bandwidths," in *Proc. 15th Int. Superconductive Electron. Conf. (ISEC)*, Nagoya, Japan, Jul. 2015, pp. 1–3.

[4] H.-W. Wu, G.-S. Chen, and Y.-W. Chen, "New compact triple-passband bandpass filter using multipath-embedded stepped impedance resonators," *IEEE Microw. Wireless Compon. Lett.*, vol. 24, no. 3, pp. 158–160, Mar. 2014.

[5] K.-W. Hsu and W.-H. Tu, "Design of a novel four-band microstrip bandpass filter using double-layered substrate," in *IEEE MTT-S Int. Microw. Symp. Dig.*, Boston, MA, USA, Jun. 2009, pp. 1041–1044.

[6] B. Ren *et al.*, "Miniature dual-band bandpass filter using modified quarter-wavelength SIRs with controllable passbands," *Electron. Lett.*, vol. 55, no. 1, pp. 38–40, 2019.
[7] H. W. Wu, L. Y. Jian, Y. W. Chen, and Y. K. Su, "New triple-passband bandpass filter using multipath stub loaded resonators," *IEEE Microw. Wireless Compon. Lett.*, vol. 26, no. 3, pp. 186–188, Mar. 2016.
[8] N. Kumar and Y. K. Singh, "Compact tri-band bandpass filter using three stub-loaded open-loop resonator with wide stopband and improved bandwidth response," *Electron. Lett.*, vol. 50, no. 25, pp. 1950–1952, 2014.
[9] C. Y. Hsu, C. Y. Chen, and H. R. Chuang, "Shunted-line stepped-impedance resonator," *IEEE Microw. Mag.*, vol. 13, no. 5, pp. 34–48, Jul. 2012.
[10] Z. Ma, T. Kawaguchi, Y. Kobayashi, D. Koizumi, K. Satoh, and S. Narahashi, "A miniaturized high temperature superconducting band-pass filter using CPW quarter-wavelength spiral resonators," in *IEEE MTT-S Int. Microw. Symp. Dig.*, San Francisco, CA, USA, Jun. 2006, pp. 1197–1200.
[11] X. L. Lu *et al.*, "Design of a high-order dual-band superconducting filter with controllable frequencies and bandwidths," *IEEE Trans. Appl. Supercond.*, vol. 24, no. 2, pp. 3–7, Apr. 2014.
[12] H. Liu *et al.*, "Triband high-temperature superconducting bandpass filters using multimode resonators," *IEEE Trans. Appl. Supercond.*, vol. 26, no. 5, Aug. 2016, Art. no. 1501506.
[13] F. Song, B. Wei, L. Zhu, Y. Feng, R. Wang, and B. Cao, "A novel tri-band superconducting filter using embedded stub-loaded resonators," *IEEE Trans. Appl. Supercond.*, vol. 26, no. 8, Dec. 2016, Art. no. 1502009.
[14] H. Liu, J. Lei, X. Guan, L. Sun, and Y. He, "Compact triple-band high-temperature superconducting filter using multimode stub-loaded resonator for ISM, WiMAX, and WLAN applications," *IEEE Trans. Appl. Supercond.*, vol. 23, no. 6, pp. 99–103, Dec. 2013.
[15] X. Guan *et al.*, "Compact triple-band high-temperature superconducting filter using coupled-line stepped impedance resonator," *IEEE Trans. Appl. Supercond.*, vol. 26, no. 7, Oct. 2016, Art no. 1501905.
[16] T. Unno and N. Sekiya, "Compact high-pole HTS triband bandpass filters using a new feeding structure," *IEEE Trans. Appl. Supercond.*, vol. 28, no. 4, Jun. 2018, Art. no. 1500305.

HAIWEN LIU (M'04–SM'13) received the B.S. degree in electronic system and the M.S. degree in radio physics from Wuhan University, Wuhan, China, in 1997 and 2000, respectively, and the Ph.D. degree in microwave engineering from Shanghai Jiao Tong University, Shanghai, China, in 2004.

From 2004 to 2006, he was a Research Assistant Professor with Waseda University, Kitakyushu, Japan. From 2006 to 2007, he was a Research Scientist with Kiel University, Kiel, Germany, granted by the Alexander von Humboldt Research Fellowship. From 2007 to 2008, he was a Professor with the Institute of Optics and Electronics, Chengdu, China, supported by the 100 Talents Program of the Chinese Academy of Sciences. From 2009 to 2017, he was a Chair Professor with East China Jiaotong University, Nanchang, China. In 2014, he joined Duke University, Durham, NC, USA, as a Visiting Scholar. In 2015, he joined the University of Tokyo, Tokyo, as a Visiting Professor, supported by the JSPS Invitation Fellowship. In 2016, he joined the City University of Hong Kong, Hong Kong, as a Visiting Professor. Since 2017, he has been a Full-Time Professor with Xi'an Jiaotong University, Xi'an, China. He has authored or co-authored more than 100 papers in international and domestic journals and conferences. His current research interests include electromagnetic modeling of high-temperature superconducting circuits, RF and microwave passive circuits, antennas for wireless terminals, radar systems, and radio telescope applications. He was a recipient of National Talent Plan, China, in 2017. He was the Executive Chairman of the National Antenna Conference of China, in 2015, and the Co-Chairman of the National Compressive Sensing Workshop of China, in 2011, and the Communication Development Workshop of China, in 2016. He has served as the Editor-in-Chief for the *International Journal of RF and Microwave Computer-Aided Engineering* (Wiley), as an Associate Editor for the IEEE Access, and as the Guest Chief Editor for the *International Journal of Antennas and Propagation*.

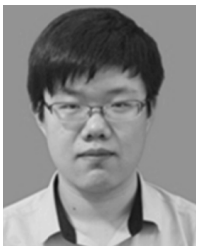

YIFAN WANG received the B.S. degree in communication engineering from East China Jiaotong University, Nanchang, China, in 2016, where he is currently pursuing the M.S. degree in communication and information system.

PIN WEN (SM'16) was born in Jiangxi, China. He received the B.S. degree in information and communication from East China Jiaotong University, Jiangxi, in 2015. He is currently pursuing the Ph.D. degree in electromagnetic field and microwave technology with Xi'an Jiaotong University, Shaanxi, China.

From 2015 to 2018, he was a Research Assistant with the Radio Frequency Communication and Sensor Network Key Laboratory of Jiangxi Province. He has authored or co-authored more than 50 internationally refereed journal and conference papers (including 31 IEEE papers). His current research interests include microwave planar filters, power dividers, and diplexers, and high-temperature superconducting planar circuits.

SHAOYONG ZHENG (S'07–M'11–SM'17) was born in Fujian, China. He received the B.S. degree in electronic engineering from Xiamen University, Fujian, in 2003, and the M.Sc., M.Phil., and Ph.D. degrees in electronic engineering from the City University of Hong Kong, Hong Kong, in 2006, 2008, and 2011, respectively, where he was a Research Fellow with the Department of Electronic Engineering, from 2011 to 2012, and a Visiting Assistant Professor with the Department of Electronic Engineering, from 2013 to 2015. He is currently an Associate Professor with the School of Electronics and Information Technology, Sun Yat-sen University, Guangzhou, China, where he is also the Deputy Director of the Mobile Communication National Engineering Research Center. He has authored or co-authored more than 100 internationally refereed journal and conference papers, including 41 IEEE Transactions papers. His research interests include microwave/millimeter wave components and evolutionary algorithms. He has served as a Technical Program Committee Member and the Session Organizer/Chair for a number of conferences, such as ICUWB, ACES, APCAP, and iWEM.